Geological model Construction for Yamama Formation at Faihaa Oil Field- South of Iraq

Zuhoor J. Younis Al-Aani[1]*, Fahad M. Al-Najm[1], Zainab A. Khalaf [2]

1. Department of Geology, College of Science, University of Basrah, Basra, Iraq.
2. Department of Mathematics, College of Science, University of Basrah, Basra, Iraq
*Corresponding Author Email: zuhoorjawad89@gmail.com

Doi 10.29072/basjs.2020310

Abstract

A construction of a 3D geological model of Yamama Formation to explain the distribution of petrophysical properties (shale volume, effective porosity and hydrocarbon saturation) by using Petrel software. Five wells were selected in order to build structural and petrophysical models based on the interpretation of well logs and petrophysical properties. Yamama reservoir is divided into four main units (YA, YB, YC, and YD), YA is divided into five secondary reservoir units (YA1, YA2, YA3, YA4, and YA5), YB is divided into two secondary reservoir units (YB1 and YB2), YC is divided into two secondary reservoir units (YC1 and YC2) and YD is divided into three secondary reservoir units (YD1, YD2, and YD3). The structural model showed Faihaa oil field represented by an anticlinal fold with double plunging. Petrophysical models (shale volume, effective porosity and hydrocarbon saturation) were constructed for each subunit of Yamama reservoir using sequential Gaussian simulations executed with Petrel software. According to data analyzes and the results from modelling, the subunits for both YB and YB are good reservoir units regarding its good petrophysical properties (high effective porosity and high hydrocarbon saturation) and are considered the most important productive units in Yamama Formation.

Article inf.

Received: 4/11/2020

Accepted 27/12/2020

Published 31/12/2020

Keywords: Geological modeling, Petrophysical properties, Yamama Formation

1. Introduction

Yamama Formation is considered as one of the most important lower cretaceous carbonate formation and main productive reservoirs in south of Iraq, that deposited during Late Tithonian-Hauterivian sequence within deposited in shoal and deep inner shelf environments as a part of the Thamama group [1]. By interpretation of well logs, Yamama Formation is divided into four main units (YA, YB, YC and YD) separated by three main caps. Yamama unit is divided into subunits based on petrophysical properties, where YA is divided into five subunits, YB into two subunits, YC into two subunits and YD into three subunits.

2. Previous Works

Yamama Formation is polarized the attention of many researchers because it is Carbonate formations of economic importance. The important studies related to the formation of Yamama are: Steinke and Bramkamp (1952) first described Yamama Formation in Saudi Arabia and stated that Yamama Formation represented as a part of the Thumama group [2]. In Iraq, Yamama formation is descripted by Dunington (1959) and Van Bellen et al. (1959), as a section with Sulay Formation underlying the argillaceous Ratawi Formation at well Ratawi-1 [3]. Eliwi et al. (2014) clarify, through the 3D geological model for Yamama units (YA, YB and YC) in Ratawi field, that YB unit is the best unit have a good petrophysical properties comparing with the other two units [4]. Jamal and Abdullah (2018) have divided Yamama Formtion at Gharaf oilfield into nine reservoir units depending on depositional facies analyses and petrophysical properties and they showed that unit Y2 is main reservoir unit characterized by high reservoir quality, while the units Y3, Y4, and Y8 have a low reservoir quality compared with other reservoir units [5]. Handhal et al. (2019) represented an evaluation method of the properties of the petrophysical in three wells in Faiha oilfield: FA-1, FA-2, and FA-3, and one from Sindibad oilfield (in well Snd-2) of Mishrif and Yamama Formations, south of Iraq. This evaluation method based on well-logs data to delineate the characteristics of the reservoir of Mishrif and Yamama formations [6]. Ahmed et al. (2020) studied the diagenesis processes for Yamama Formation by core examination and clarified there are eight diagenetic processes showed positive and destructive effects on quality of the reservoir [7]. In this study, we focus on Faihaa field, which considered a new field, with a lack of studies about Yamama reservoir within Faihaa field.

3. Study Area

Faihaa field is an anticline fold located in the north-east of the Block 9 north of Basra in south of Iraq at the southeastern part of Mesopotamian basin within Zubair subzone. And distance around 20 km north of Basrah adjacent and parallel to Iraq-Iran borders as shown in figure (1). Bounded in north by Majnon field and from the south by Sindbad field and from the west Nahr Omar and from the east Iranian Hosseinieh field [8].

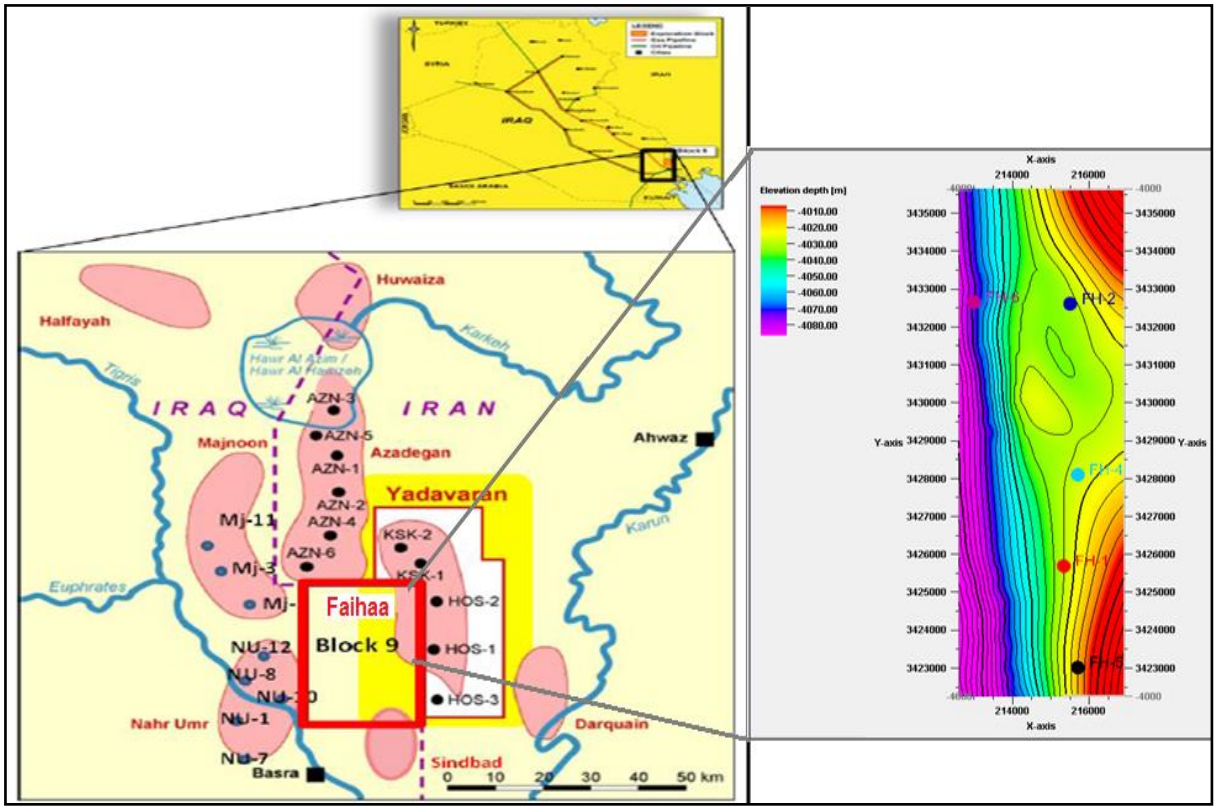

Figure 1: Location map of study area (Fiahaa Field).

4. Tectonic Setting and Stratigraphy

Jassim & Goff (2006) [9] indicated that the Late Tithonian – Early Turonian Megasequence (AP8) are deposited in a large intra – shelf basin with a new phase of ocean floor spreading in Southern Neo-Tethys. The opening of Southern Neo-Tethys led to drifting of a narrow microcontinent away and a new passive margin formed along the North East to margin of Arabian Plate. Rutbah uplift formed in the west of margin for Mesopotamian Basin, while the North East margin formed by a carbonate ridge along the north passive margin of Southern Neo-Tethys. Yamama Formation belongs to the late Berriasian-Aptian cycle [10]. This cycle

is referred to from shore to deep basin by Zubair, Ratawi, Garaga, Yamama, Shuiaba, Sarmord, and lower Balambo Formations. The bottom of Yamama Formation passes into and overlies Sulaiy Formation and in top overlies conformably with Ratawi Formation [1]. The eastern margin of the basin may be formed by a carbonate ridge which bordered the continental margin along the southern Neo-Tethys [9].

5. Materials and methods

1. In the Faihaa oil field, five wells from the Yamama formation were selected to cover the study area, which included: FH-1, FH-2, FH-4, FH-5 and FH-6.
2. The data collected from the studied wells are gamma ray, resistivity and porosity logs were used for the calculation of petrophysical properties.
3. Using Techlog software (2015.4) to analyze and calculate petrophysical properties.
4. Build 3D geological and petrophysical models by using Petrel software (2017.4).

6. Calculating Petrophysical Properties

The equations below are used for calculating reservoir properties of Yamama Formation in order to export to Petrel software, which includes:

6.1 Shale volume (Vsh)

To derive Vsh from gamma ray (GR_{Log}), the gamma ray index (I_{GR}) is imperative to determine by using the equation of Schlumberger (1974) [11].

$$I_{GR} = (GR_{log} - GR_{min}) / (GR_{max} - GR_{min}) \quad (1)$$

Where GR_{log} is gamma ray reading of formation, GR_{min} is the minimum gamma ray reading (clean carbonate), and GR_{max} is maximum gamma ray reading (shale). Volume of shale is then determined by using the formula of Dresser Atlas [12] for older rocks as follows:

$$Vsh = 0.33 * [2^{(2*IGR)} - 1] \quad (2)$$

6.2 Porosity

The porosity of Yamama Formation is determined from a combination of Neutron – Density derived porosities. Neutron porosity corrected for shale effect by using the equation of Tiab & Donaldson (2015) [13].

$$Ø_{Ncorr} = Ø_N - (V_{sh} * ØN_{sh}) \quad (3)$$

Where $Ø_{Ncorr}$. is the corrected Shale-corrected neutron porosity, $Ø_N$ is the Neutron porosity reading direct from neutron log, and $Ø_{Nsh}$ is Neutron porosity for shale.

Porosity is determined from the density log using Wyllie et al. (1958) equation [14] when the matrix density (ρ_{ma}) and the density of the saturating fluids (ρ_f) are known as below:

$$\emptyset_D = (\rho_{ma} - \rho_b) / (\rho_{ma} - \rho_f) \quad (4)$$

Where ρ_{ma} is the density of matrix (2.71 gm/cm^3 for limestone, ρ_f = density of fluid 1.1 gm/ cm^3 for saline water).

Density porosity is corrected from the effect of the shale for intervals with a shale ratio of more than 10%, using equation (Dresser Atlas, 1979) [12].

$$\emptyset_{D\_corr} = \emptyset_D - (V_{sh} * \emptyset D_{sh}) \quad (5)$$

Where $\emptyset_{Dcorr}$. is the corrected porosity derived from the density log for dirty rocks**,** and $\emptyset_{Dsh}$ is density porosity for shale.

Porosity from Neutron-Density log can be calculated mathematically by using the following equation:

$$\emptyset_{N.D} = (\emptyset_N + \emptyset_D) / 2 \quad (6)$$

Corrected Neutron – Density porosity for shale effect can be calculated by using the equation of Schlumberger (1998) [15]

$$\emptyset_{N.D\_corr} = ((\emptyset_{N\_corr}) + (\emptyset_{D\_corr}))/2 \quad (7)$$

6.3 Water and hydrocarbon saturation

Water saturation for the uninvaded zone is calculated according to Archie (1942) [16]:

$$Sw = \{(a * Rw) / (Rt * \emptyset^m)\}\ 1/n \quad (8)$$

In depth intervals of shale volume (V_{sh}) more than 10 is calculated by using the equation of Simandoux, 1963 [17]:

$$S_w = [0.4 * R_t / \emptyset^2_{corr} * \sqrt{[\{(V_{sh}/R_{sh})^2 + (5 * \emptyset^2 / R_w * R_t)\}]} - (V_{sh}/R_{sh})] \quad (9)$$

Where S_w is water saturation, Ø is Neutron – Density porosity, R_t is true formation resistivity, $\emptyset_{corr}$ is corrected Neutron – Density porosity, R_{sh} is Resistivity of shale. R_w value and the coefficient (a, m, n) can calculate from Pickett plot and as the following equation that shown in figure (2) [18].

$$Log\ (Rt) = -\ m \log (\emptyset) + \log (a.\ Rw) \quad (10)$$ (In water-bearing zone, Sw = 1)

Where Rw is resistivity of water formation, a is tortuosity factor; m is cementation factor and n is saturation exponent.

Then the hydrocarbon saturation can be calculated by using the following equation:

$$Sh = 1 - Sw \quad (11)$$

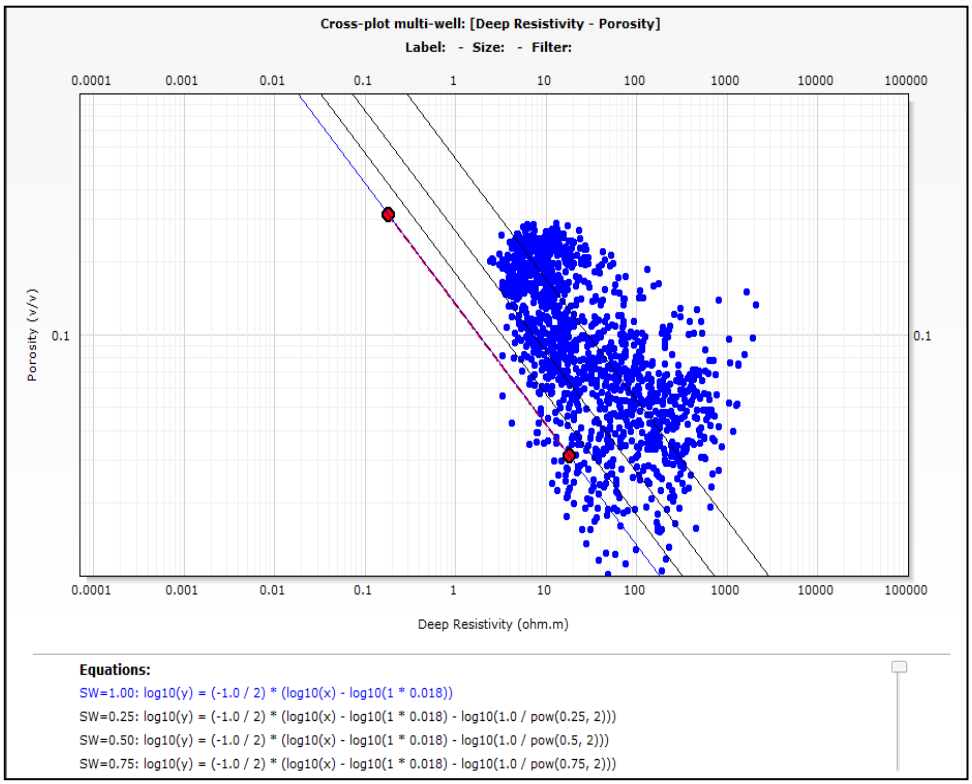

Figure 2: The results of Pickett plot in well FH-1.

7. Geological Modeling

7.1 Structural Model

In order to make structural model, a structure contour map must be available which represents the most important tools for three-dimensional structural interpretation. 3D Structural maps were built depending on structural contour map and the well tops for all Faihaa wells. Structural modeling is subdivided into two follows processes: edit polygon and made the surface. 3D contour structures are built for each unit of Yamama Formation as shown in Fig.3.

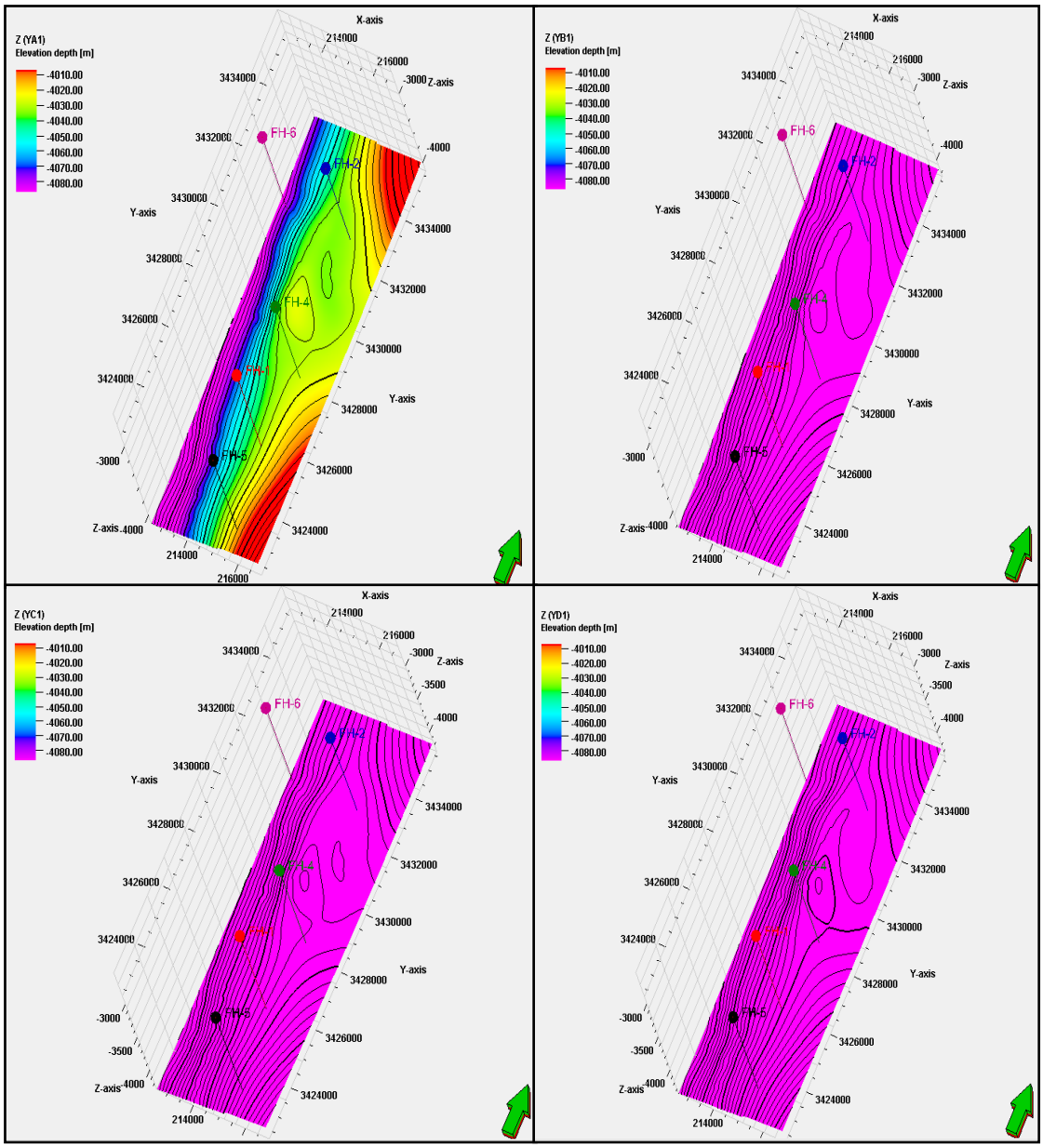

Figure 3: 3D structural modeling of Yamama units (YA, YB, YC and YD) at Faihaa oilfield.

7.2 Well log Scaling-up

The scale-up well logs process averages the values of the cells in the 3D grid that are penetrated by the wells. There are many statistical methods used in measurement such as (arithmetic, harmonic, and geometric method) [19]. The values of shale volume, effective porosity and hydrocarbon saturation in the current model scaled up by using (arithmetic mean). Figure (4) shows the scale-up of shale volume, effective porosity and hydrocarbon saturation for five study wells that are used in the Yamama Formation model.

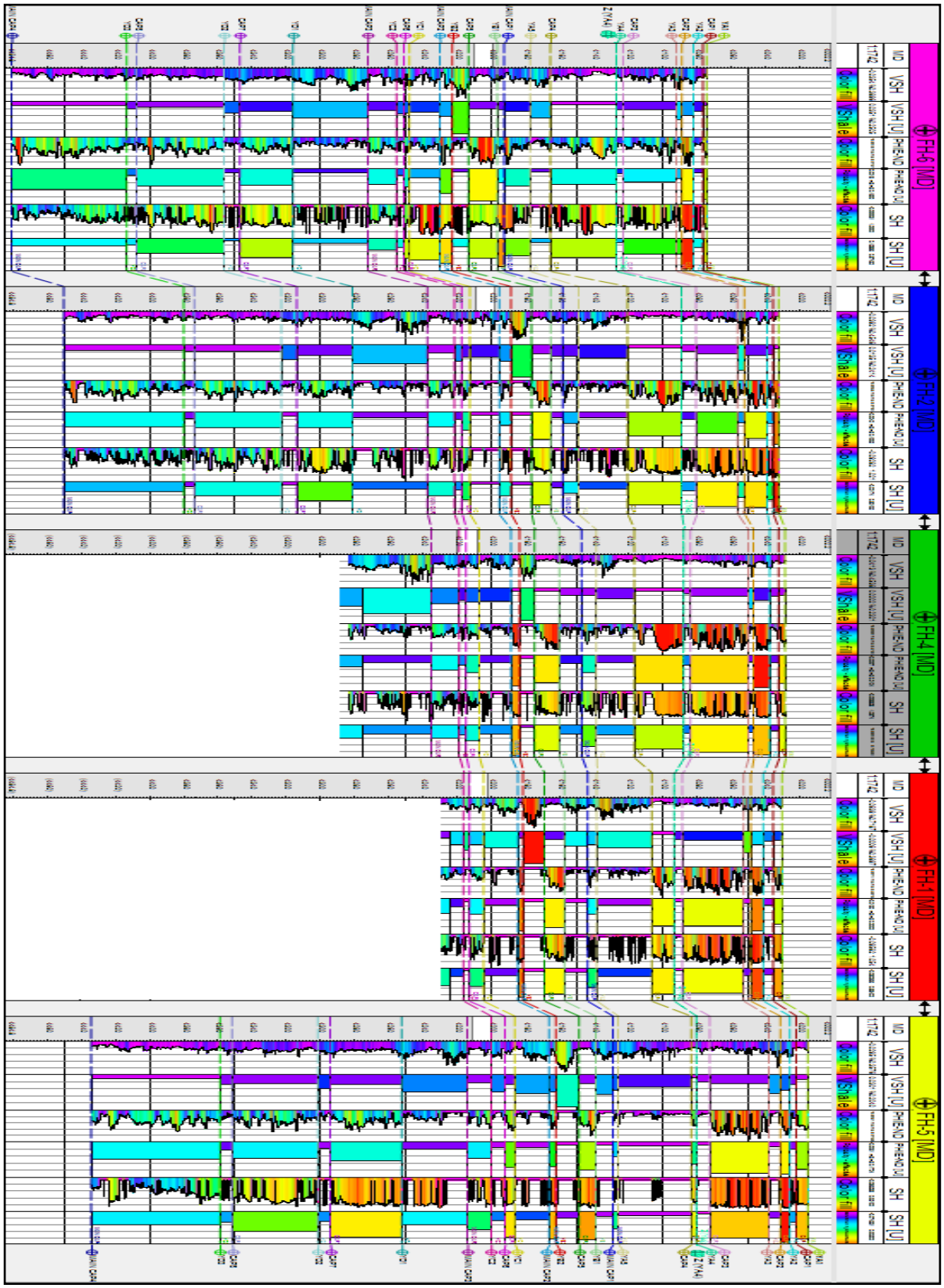

Figure 4: Scale up of shale volume, effective porosity and hydrocarbon saturation for study wells.

7.3 Petrophysical Model

Petrophysical model reflects the distribution of petrophysical properties which change in each zone of Yamama Formation with depth along Faihaa field. Petrophysical properties model that results from the output of logging process interpretation CPI of Yamama reservoir which includes: Shale volume, effective porosity and hydrocarbon saturation which are corrected and interpreted in Techlog software as shown in table (1). Petrel offers several algorithms for modeling the distribution of petrophysical properties in a reservoir model [20]. In this study, the petrophysical model is created by using the sequential Gaussian simulation as executed in Petrel.

Table 1: Average values of petrophysical properties of the study wells.

Subunit	FH-1			FH-2			FH-4			FH-5			FH-6		
	Avg Vsh	Avg $\emptyset_e$	Avg S_H	Avg Vsh	Avg $\emptyset_e$	Avg S_H	Avg Vsh	Avg $\emptyset_e$	Avg S_H	Avg Vsh	Avg $\emptyset_e$	Avg S_H	Avg Vsh	Avg $\emptyset_e$	Avg S_H
YA1	0.1	0.14	0.75	0.04	0.19	0.82	0.06	0.17	0.68	0.06	0.13	0.73	0.06	0.15	0.68
YA2	0.15	0.19	0.82	0.09	0.15	0.7	0.09	0.2	0.77	0.11	0.16	0.82	0.12	0.16	0.82
YA3	0.1	0.15	0.66	0.07	0.12	0.68	0.07	0.16	0.7	0.07	0.15	0.76	0.09	0.08	0.57
YA4	0.03	0.15	0.67	0.03	0.13	0.63	0.04	0.16	0.72	0.04	0.1	0.66	0.05	0.1	0.65
YA5	0.14	0.08	0.53	0.09	0.06	0.63	0.07	0.1	0.53	0.11	0.07	0.57	0.1	0.09	0.58
YB1	0.09	0.16	0.67	0.07	0.15	0.62	0.04	0.16	0.62	0.07	0.14	0.75	0.08	0.16	0.70
YB2	0.07	0.18	0.77	0.12	0.07	0.46	0.03	0.2	0.73	0.12	0.12	0.75	0.13	0.12	0.69
YC1	0.14	0.08	0.46	0.09	0.1	0.47	0.11	0.1	0.37	0.08	0.12	0.68	0.11	0.09	0.58
YC2	0.06	0.09	0.5	0.07	0.08	0.38	0.11	0.08	0.31	0.07	0.08	0.67	0.09	0.09	0.41
YD1	-	-	-	0.08	0.08	0.52	-	-	-	0.08	0.09	0.72	0.09	0.09	0.59
YD2	-	-	-	0.06	0.09	0.36	-	-	-	0.07	0.08	0.6	0.07	0.09	0.5
YD3	-	-	-	0.05	0.08	0.27	-	-	-	0.05	0.08	0.39	0.06	0.11	0.33

7.3.1 Shale Volume models

The colors (red, yellow and green) in figures (5 to 7) indicate the shale volume increasing, while the colors (cyan, blue and purple) indicate the shale volume with low values. From figures (5 to 7), can notice that the average of shale volume in all study wells not exceed (17%). In FH-

1well, notice that shale volume is increasing, especially in subunits (YA2, YA5 and YC1), while (YA4) has the lowest value of shale volume at all study wells with a value not exceed (5%). Also, the FH-2, FH-5 and FH-6 wells have a low value within subunits (YA1, YA4, YD1 and YD2), while the values increasing within (YA5 and YB2). In contrast, FH-4 well records a highest value of shale volume in (YC1 and YC2) and a lowest value within (YA4, YB1 and YB2).

7.3.2 Effective Porosity models

Figures (8 to 10) show the distribution of effective porosity in Yamama reservoir subunits. Colors (red, yellow and green area) are indicators of the good effective porosity which range between (20%-12%) especially in well FH-4 that has the highest porosity in all subunits. While in FH-2, this property increased in subunits (YA1, YA2, and YB1). Well FH-5 contains good effective porosity in subunits (YA2, and YA3), while well FH-1 has good porosity only within (YA2, and YB1). The (cyan, blue and purple) colors are characterized as a poor effective porosity in the model and as following: well FH-6 is ranged between (7%-9%) within subunits (YA5, YC2, YD1, and YD2), while the wells FH-1and FH-4 in subunits (YA5 and YC2) and wells FH-1, FH-4 in subunit (YA5, YC2, YD1, YD2, YD3) include the values of effective porosity ranged between (10%-8%).

7.3.3 Hydrocarbon saturation models

Figures (11 to 13) show the distribution of hydrocarbon saturation in Yamama reservoir subunits can be shown. The colors (red, yellow, and green) are indicators of the good values greater than (50%) while the colors (cyan, blue and purple) indicate the hydrocarbon saturation is less than (50%). Well FH-5 shows the higher hydrocarbon saturation in the subunits (YA1, YA2, YA3, YB1, and YB2) with average (82%-73%). While in FH-2, the hydrocarbon saturation increased in (YA1, YA2, and YB1) and decreased in (YA5, YC2, YD1, YD2, and YD3) subunits. FH-1 well contains a hydrocarbon saturation which increased in subunits (YA1, YA2, and YB2) with an average (82%-75%) and decreased within (YA5, YC1, and YC2). FH-4 well has a good hydrocarbon saturation value within (YA1, YA2, YA3, and YA4) with an average of (70%-77%), while well FH-6 shows increasing in hydrocarbon saturation in subunits (YA2, YB2) with an average (70%-82%). Both FH-5 and FH-6 show a decrease in hydrocarbon saturation values within (YD3) subunit.

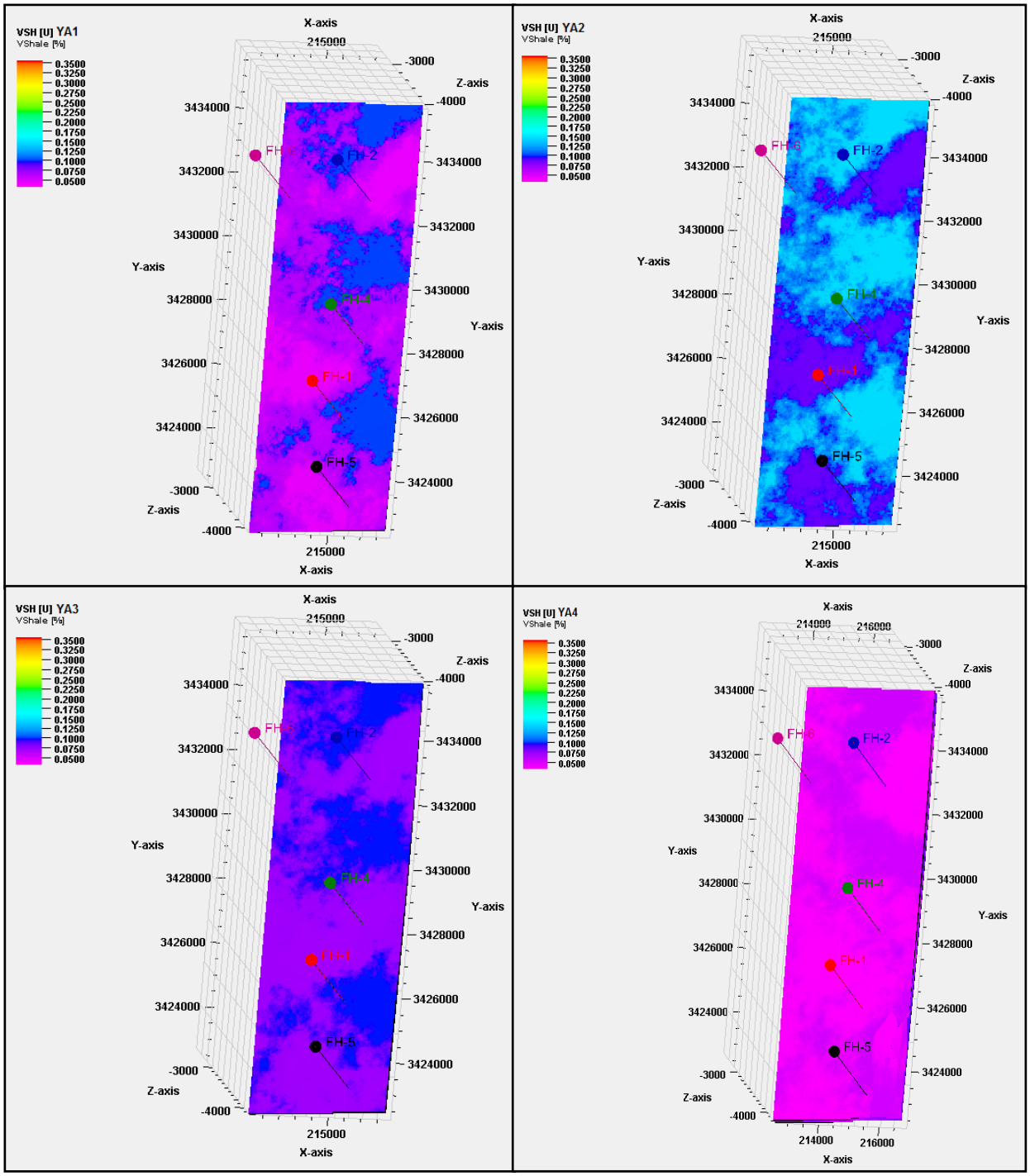

Figure 5: 3D model for shale volume distribution throughout Yamama reservoir subunits (YA1, YA2, YA3 and YA4)

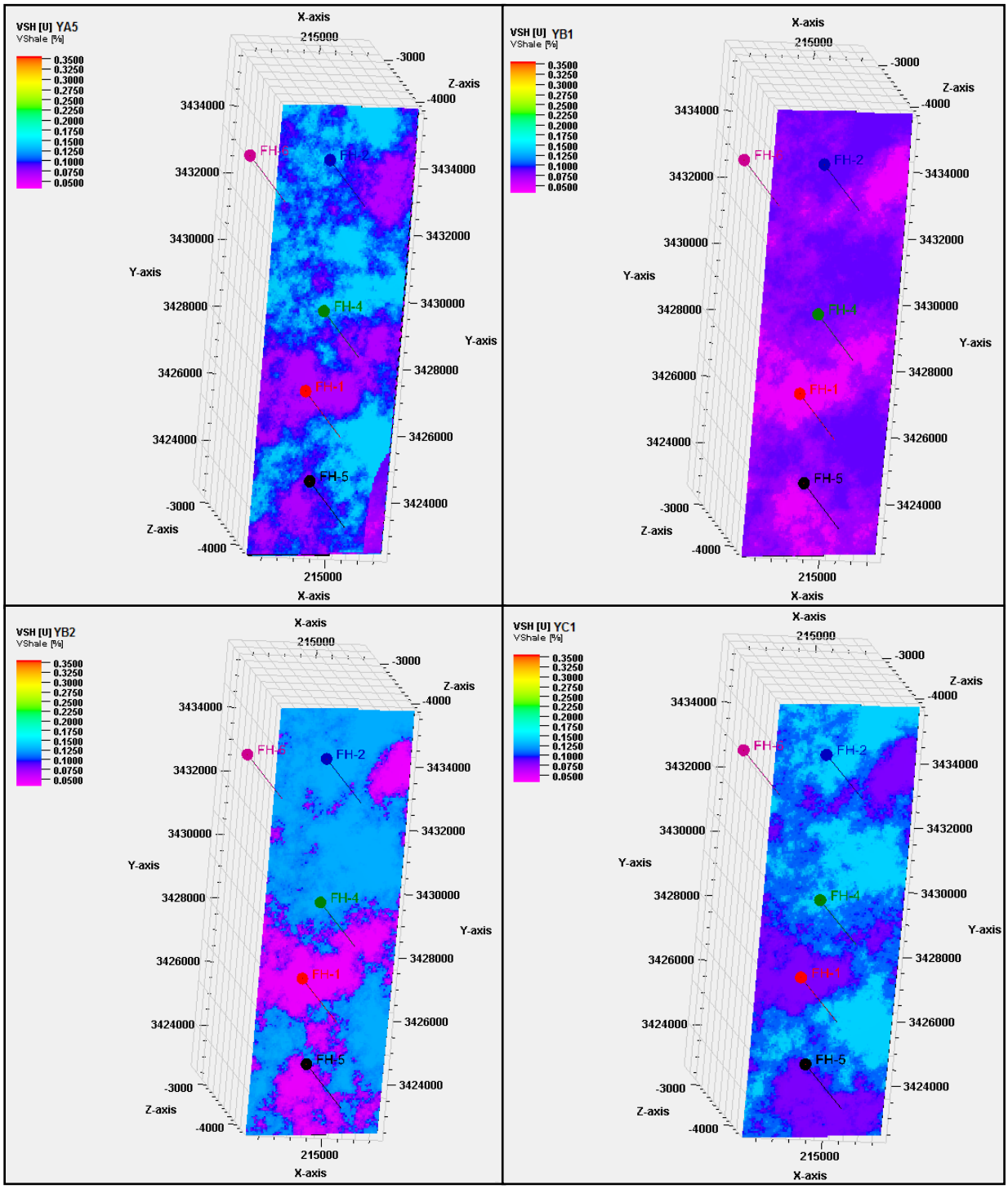

Figure 6: 3D model for shale volume distribution throughout Yamama reservoir subunits (YA5, YB1, YB2 and YC1)

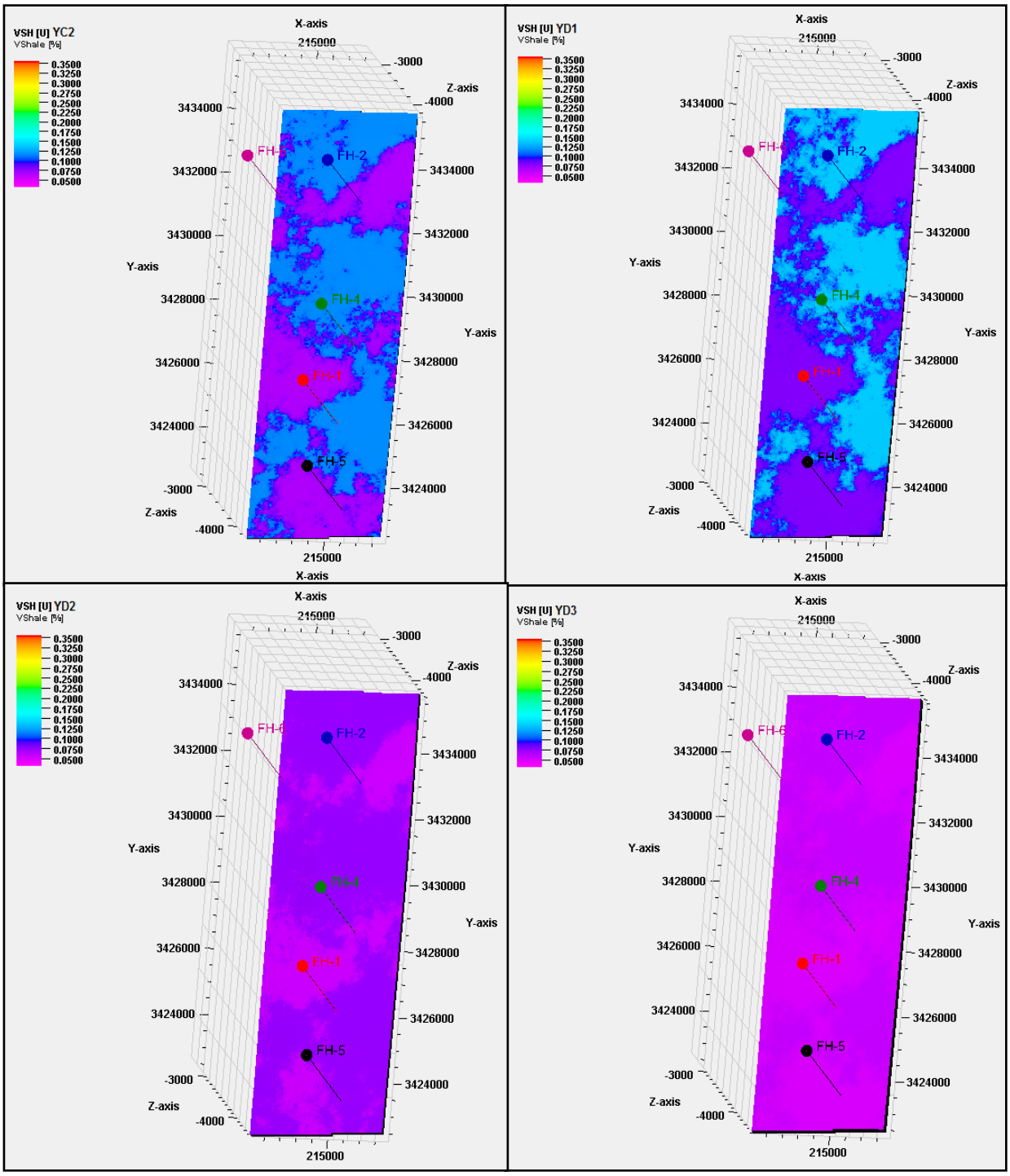

Figure 7: 3D model for shale volume distribution throughout Yamama reservoir subunits (YC2, YD1, YD2 and YD3).

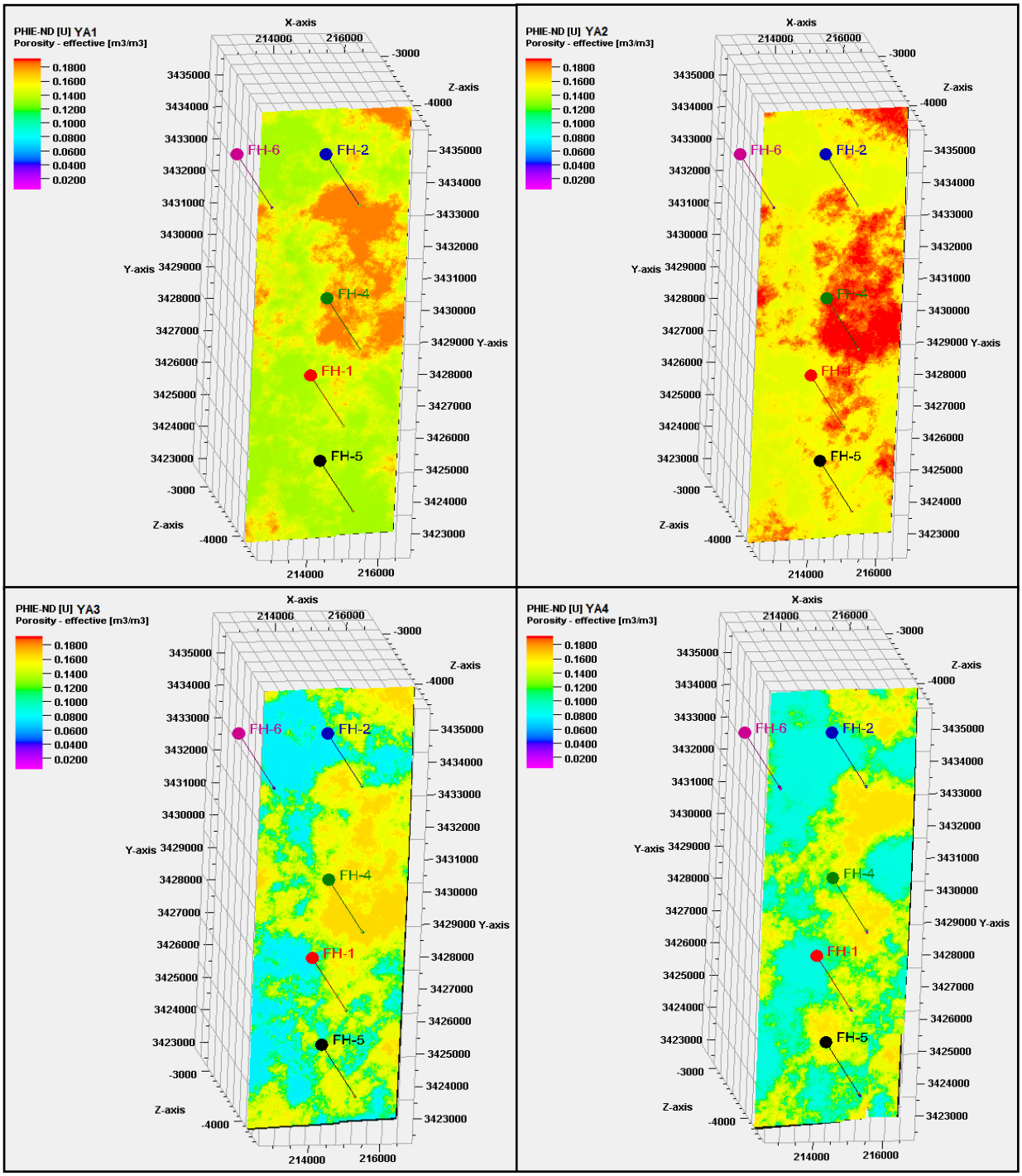

Figure 8: 3D model for effective porosity distribution throughout Yamama reservoir subunits (YA1, YA2, YA3 and YA4).

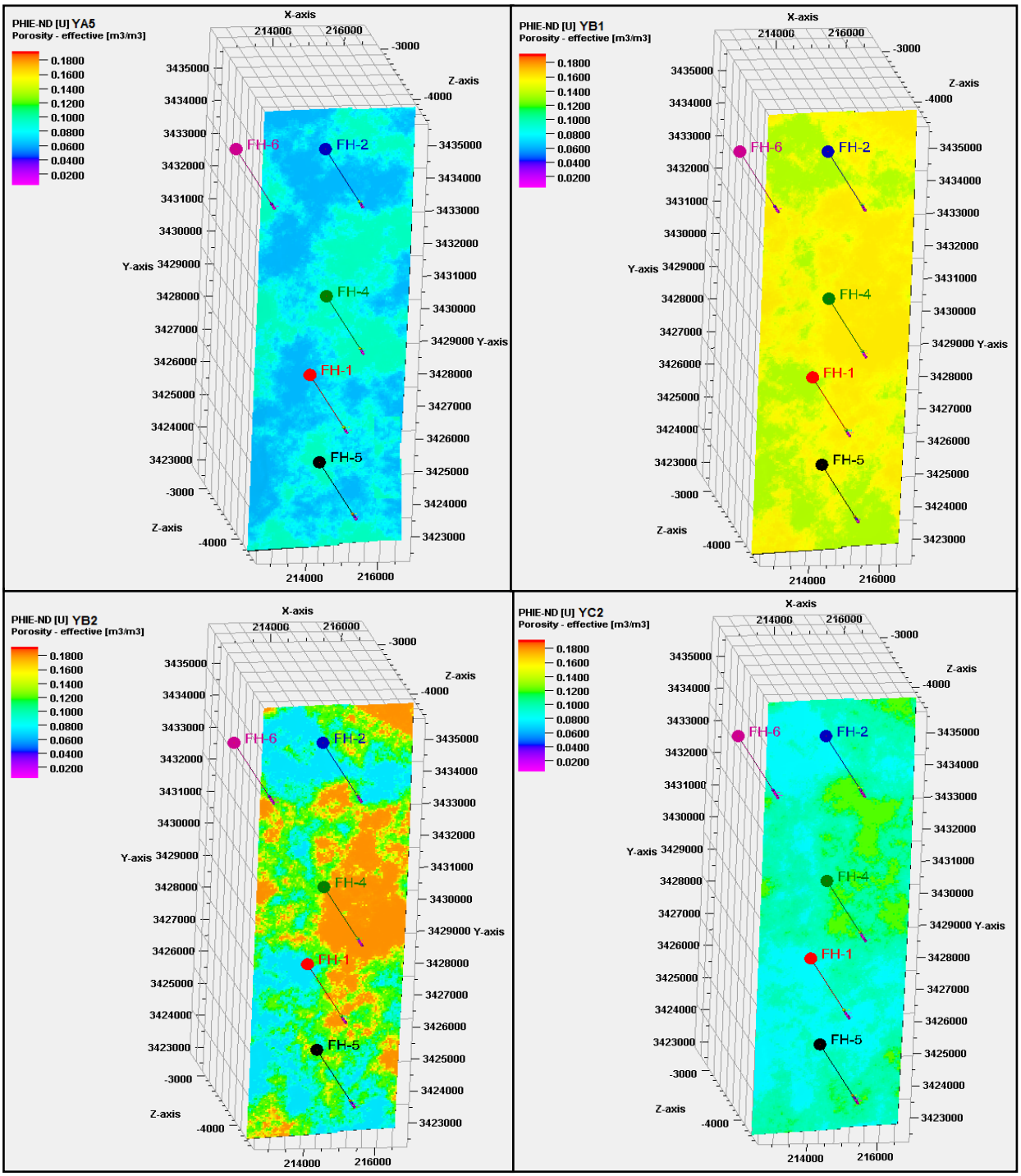

Figure 9: 3D model for effective porosity distribution throughout Yamama reservoir subunits (YA5, YB1, YB2 and YC1).

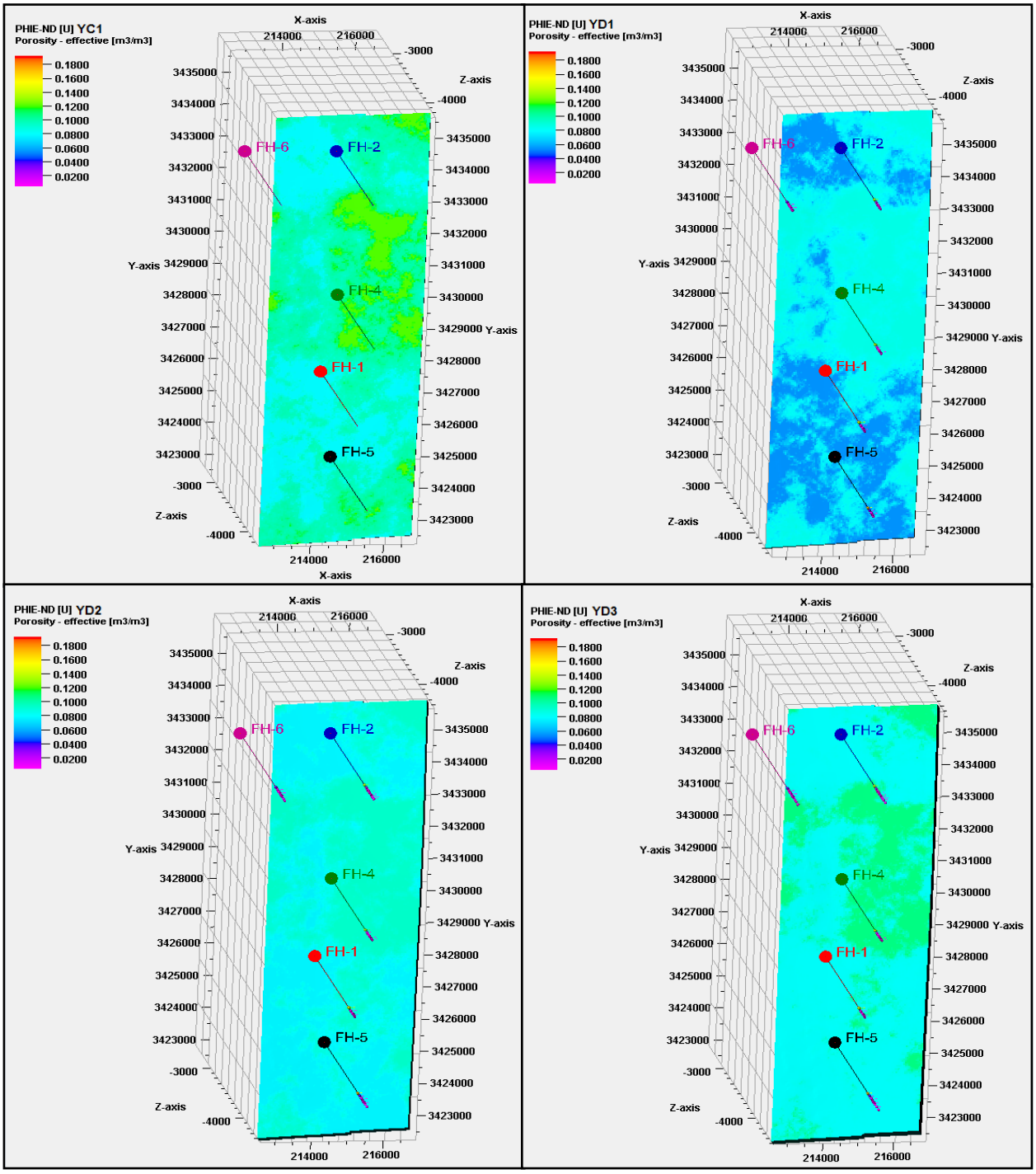

Figure 10: 3D model for effective porosity distribution throughout Yamama reservoir subunits (YC2, YD1, YD2 and YD3).

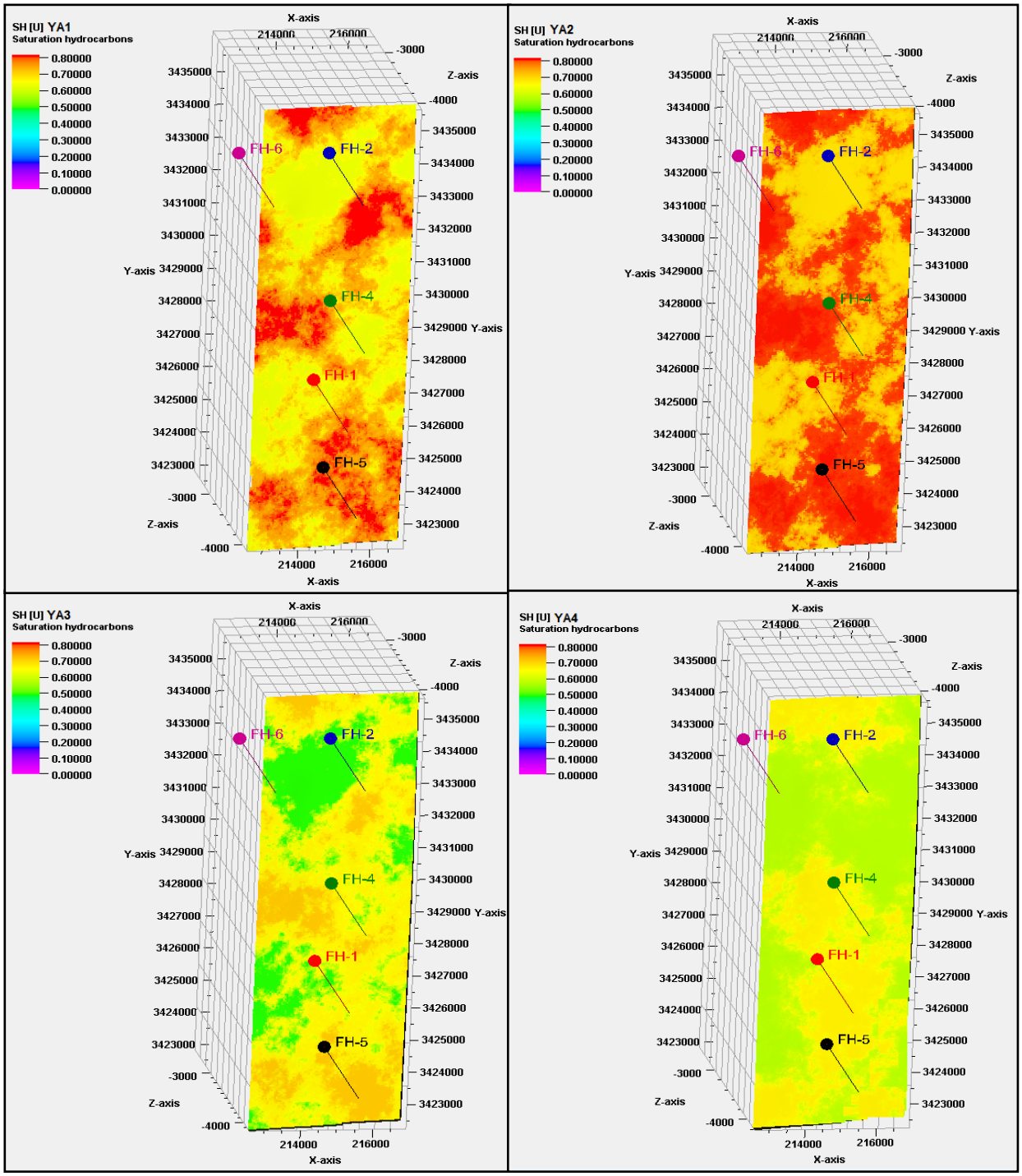

Figure 11: 3D model for hydrocarbon saturation distribution throughout Yamama reservoir subunits (YA1, YA2, YA3 and YB1).

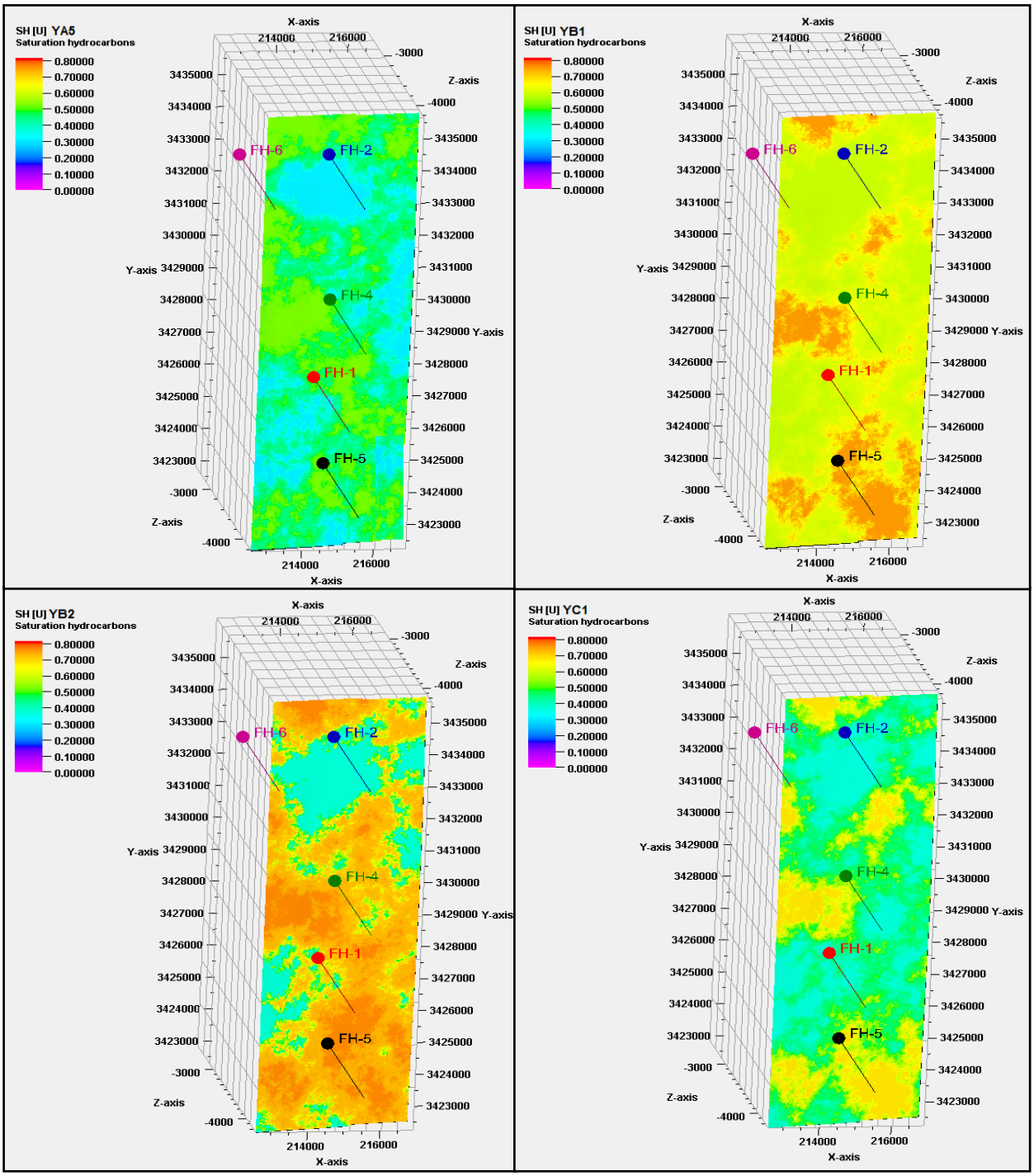

Figure 12: 3D model hydrocarbon saturation distribution throughout Yamama reservoir subunits (YA5, YB1, YB2 and YC2).

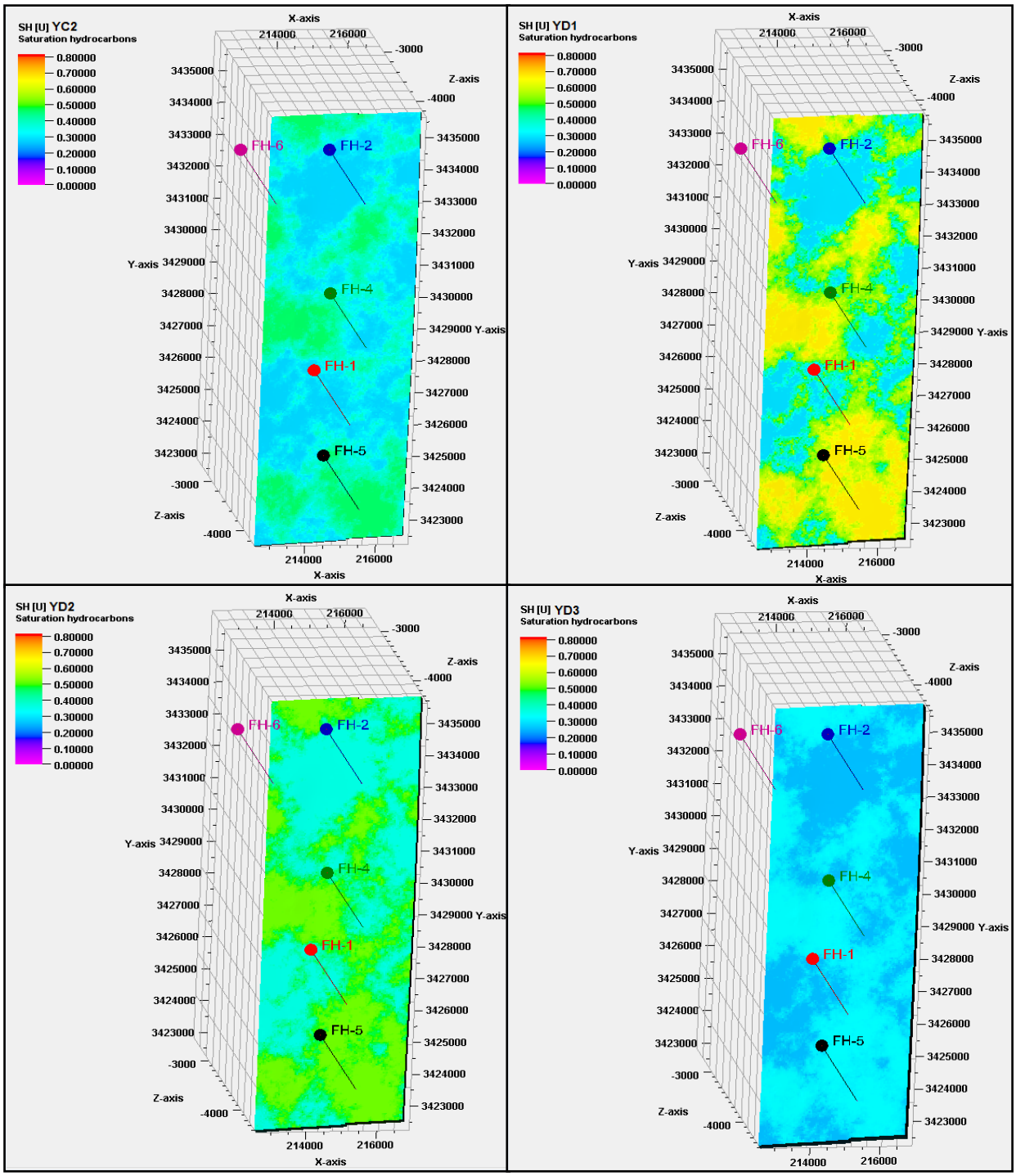

Figure 13: 3D model for hydrocarbon saturation distribution throughout Yamama reservoir subunits (YC2, YD1, YD2 and YD3).

8. Conclusions

By analyzing the shale volume, effective porosity and hydrocarbon saturation models for each reservoir subunit of Yamama Formation, the following conclusions can be shown:

- The studied model shows the high value for effective porosity and hydrocarbon saturation are occurring in the subunits (YA1, YA2, YA3, YA4, YB1, and YB2), which represents the important oil bearing subunits.
- The reservoir subunits YA5, YC1, YC2, YD1, YD2, and YD3 are characterized by moderate to poor petrophysical properties.
- The FH-4 is characterized by good reservoir properties which are located on the crest of Faihaa structure.
- Faihaa structure, it is a sample and symmetrical anticline with double plunging.

References

[1] F. N. Sadooni, Stratigraphie Sequence, Microfacies, and Petroleum Prospects of Yamama Formation, Lower Cretaceous, South of Iraq, AAPG bulletin, 11 (1993) 1971-1988.

[2] Steinke and R. A. Bramkamp, Mesozoic rocks of east of Saudi Arabia (abs.), AAPG Bulletin, 36 (1952) 909.

[3] R.C. Bellen, H.V. Dunnington, R. Wetzel, and D.M. Morton, Lexique stratigraphic international, CNRS, 1959.

[4] N. Eliwi, G. Hassan and N. Shihab, Evaluation of the Petrophysical Properties of Yamama Formation in Ratawi oil field, South of Iraq, Iraqi Journal of Science, 55 (2014) 1891-1901.

[5] S. Jamal, T. Abdullah, Reservoir Units of Yamama Formation in Gharafoilfiled, South of Iraq, Iraqi Journal of Science, 59 (2018) 697-710.

[6] A. Handhal, H. Chafeet, N. Dahham and R. Basher, Study of Petrophysical Properties of Mishrif and Yamama Formations at Selected Fields South of Iraq, Journal Of Basrah Researches, 45 (2019) 131-161.

[7] M. Ahmed, M. Nasser and S. Jawad, Diagenesis Processes Impact on Reservoir Quality in Carbonate Yamama Formation/Faihaa Oil Field, Iraqi Journal of Science, 202 (2020) 92- 102.

[8] United Energy Group Limited, Complete Person's report on the Oil, Gas and Condensate Assets of Kuwait Energy plc, Published report, 2018.

[9] S.Z. Jassim, J. C. Goff, Geology of Iraq, Dolin-Prague and Moravian museum, Brno, 2006.

[10] T. Buday, The Regional Geology of Iraq: Stratigraphy and Paleogeography, Dar Al- Kutib house, University of Mosul, Mosul, Iraq, 1980.

[11] Schlumberger, Log Interpretation, II-Applications, New York, 1974.

[12] A. Dresser, Log Interpretation Charts, Dresser Industries, Houston, 1979.

[13] D. Tiab, E. C. Donaldson, Petrophysics: Theory and Practice of Measuring Reservoir Rock and Fluid Transport Properties, Fourth Ed, Elsevier, Amsterdam, 2015.

[14] M. R. J. Wyllie, A. R. Gregory and H. F Gardner., An experimental investigation of factors affecting elastic wave velocities in porous media, SEG, 23 (1958) 459-493.

[15] Schlumberger, Log interpretation principles / Applications, Schlumberger Wireline & Testing, 1998.

[16] G. E. Archie., The electrical resistivity logs as an aid in determining some reservoir characteristics, Transactions of the AIME, 146 (1942) 54-62.

[17] C. Bardon & B. Pied, Formation Water Saturation in Shaly Sands: SPWLA 10th Ann. Log. Symp. Trans, 1969.

[18] G. R. Pickett, A Review of Current Techniques for Determination of Water Saturation From Logs, Journal of Petroleum Technology, 18 (1966) 1425-1433.

[19] Schlumberger, Petrel Geology and Modeling, Norway, 2007.

[20] Schlumberger, Petrel Geology and Modeling, Norway, 2005.

بناء موديل جيولوجي لتكوين اليمامة في حقل الفيحاء النفطي جنوب العراق

زهور جواد يونس العاني[1]، فهد منصور النجم[1] , زينب علي خلف[2]

[1] قسم علم الارض ، كلية العلوم ، جامعة البصرة ،البصرة، العراق.
[2] قسم علم الرياضيات ، كلية العلوم ، جامعة البصرة ،البصرة، العراق.

الخلاصة

بناء نموذج جيولوجي ثلاثي الأبعاد لتكوين اليمامة لتوضيح توزيع الخصائص البتروفيزيائية (حجم السجيل ,المسامية الفعالة والتشبع الهيدروكربوني) باستخدام برنامج Petrel. تم اختيار خمسة آبار من أجل بناء النموذج التركيبي وبتروفيزيائية بناءا على تفسير سجلات الابار والخصائص البتروفيزيائية. ينقسم مكمن اليمامة إلى أربع وحدات رئيسية (YA و YB و YC و YD). YA مقسم إلى خمس وحدات مكمنية ثانوية وينقسم YB إلى وحدتين مكمنتين ثانويتين والوحدة YC إلى وحدتين مكمنتين ثانويتين والوحده YD إلى ثلاث وحدات مكمنية ثانوية . أظهر النموذج الهيكلي أن حقل الفيحاء النفطي يمثل طية منحنية مع غطس مزدوج. تم بناء النماذج البتروفيزيائي (حجم السجيل, المسامية الفعالة والتشبع الهيدروكربوني) ولكل وحده فرعية من مكمن اليمامة باستخدام محاكاة متسلسلة كاوس تم تنفيذها باستخدام برنامج بترل. وفقا لتحليلات البيانات والنتائج فان كلا الوحدات المكمنية الفرعية YB و YB هي وحدات مكمنية جيدة فيما يتعلق بخصائصها البتروفيزيائية (مسامية عالية الفعالية وتشبع هيدروكربوني عالي) ويعتبرن من أهم الوحدات الإنتاجية لتكوين اليمامة .